Hindawi
Shock and Vibration
Volume 2022, Article ID 2983700, 18 pages
https://doi.org/10.1155/2022/2983700

Research Article

Study on Vibration Control and Parameters Influence of Cable Inerter Viscous Damping System

Ruoyu Zhang[1] and Meigen Cao[2]

[1]*School of Mechanics and Engineering Science, Shanghai University, Shanghai 200444, China*
[2]*School of Civil Engineering, North China University of Technology, Beijing 100144, China*

Correspondence should be addressed to Meigen Cao; caomeigen@ncut.edu.cn

Received 4 November 2021; Revised 18 February 2022; Accepted 21 February 2022; Published 20 April 2022

Academic Editor: Zhitao Yan

In this study, a single-degree-of-freedom (SDOF) model with cable inerter viscous damper (CIVD) is established, and the vibration control equations and frequency response functions are established. Then, the influence of parameters, including inertia mass ratio, additional damping ratio, and stiffness ratio, is studied. Finally, the dynamic time history analysis of SDOF with CIVD under earthquake and fluctuating wind load is carried out to verify the damping performance of CIVD. The research shows that the additional mass and damping of CIVD can be amplified hundreds of times through the rotation, so as to realize the lightweight and high efficiency of the damper and make up for the engineering defects of the traditional TMD system. Meanwhile, when designing CIVD, the inertia mass ratio and additional damping ratio should be reduced as much as possible under the condition of meeting the target damping ratio. The CIVD can significantly suppress the resonance response of the structure and the continuous vibration response in the stable state. The peak displacement can be reduced by 30%–50%. Installing the cable and inerter element can control only the structural vibration, but it cannot reduce the amplitude in the steady state. The CID can control the inertial force output of the original structure, but the rotating speed of the inerter element is high, and the shaking speed of the original structure is fast. Therefore, in order to control the acceleration, velocity, and displacement of the original structure at the same time, we must add the appropriate inerter, additional damping, and additional stiffness.

1. Introduction

Building and lifeline structures have high vulnerability under earthquake and fluctuating wind load [1], such as super-high structures, industrial plants, and transmission tower line systems [2]. The main reason is that the natural vibration frequency of the structure is close to the predominant frequency of external excitation [3], resulting in the amplification of vibration response [4], so the vibration mitigation and control of the structure are particularly important. Therefore, many researchers have studied reinforcement measures and energy dissipation devices for reducing wind-induced or seismic response and the design methods of these devices for vibration control of different structures [5, 6]. At present, TMD is the most widely used [7], and it is applied to varying degrees in the fields of electronics, machinery, building, and so on [8]. Although electronic and mechanical equipment have higher requirements for the accuracy and robustness of vibration control than building structures, because the weight, size, and height of building structures and other special structures are much larger than other equipment and they are exposed to the external environment for a long time [9], the load conditions are more complex [10]. To achieve a certain vibration control effect, TMD needs a larger size and mass [11]. Many high-rise structures and super high-rise structures adopt the TMD design scheme. Although the wind-induced vibration control is good, the volume of TMD is large due to the large mass of the original structure itself. However, from the perspective of economy and applicability, this is unrealistic for many structures, such as high-rise space truss structures like transmission towers. The

structure itself is flexible, and the towers in the tower line system are coupled with conductor and ground cable strongly during vibration. For structures with a large mass participation coefficient during vibration, it is difficult to realize large-scale vibration mitigation measures based on TMD in areas with frequent earthquakes or typhoon transit. Therefore, it is necessary to design a lightweight and efficient damping system, which is easy to install and has little impact on the original structure.

In recent ten years, the electromechanical similarity theory [12] has provided a theoretical basis for the proposal of inerter element, and the vibration mitigation and isolation technology has been developed based on the inerter element. Compared with the traditional TMD, the damper with the inerter element can directly and effectively control the inertial force at the two terminals. Moreover, the inerter element can effectively enlarge the small actual mass through methods such as ball screw to convert the translational motion into rotary motion. In 2001, Smith [13] puts forward the concept of inerter element based on electromechanical similarity theory, gives the basic forms of ball screw inerter element and rack and pinion inerter element, and designs hydraulic inerter element in 2013 [14], which has a simpler structure and stronger robustness. Subsequently, shock absorbers were developed based on different inerter element connection forms, such as tuned viscous mass damper (TVMD) with mass element in parallel with damping element and tuned inerter damper (TID) with stiffness element in parallel with damping element. At the same time, the design method of inerter system is also studied. Ikago et al. [15] derived a simple formula for TVMD optimization design based on fixed-point theory. *Pan* et al. [16] studied the parameters of single-degree-of-freedom structures with different inerter systems, considering the natural damping of the original structure and the output cost control of the damper and making up for the deficiency of the design method based on the fixed-point theory, and proposed the design method of SPIS-II inerter damping system [17]. Hwang et al. [18] proposed a ball screw inerter system connected with a toggle brace. Through theoretical analysis and numerical calculation, it is shown that the system can be effectively used in the structure even when the drift is very small. Zhang et al. [19–21] applied the inerter damper system to high-rise structures such as chimneys and wind power towers, made a systematic theoretical analysis and parameter influence analysis, and proved the effectiveness of the inerter damping system in high-rise structures. Gao et al. [22] put forward an optimum design procedure of VID based on the output feedback control theory for controlling specific cable mode vibrations.

At present, although some Japanese scholars have used the inerter damping support in practical engineering [23], most of the research on the inerter damping system are still in the stage of theoretical analysis and numerical simulation, only the simplified mechanical model is used for the damping analysis of various structures, and only a few scholars have proposed the connection mode and design method of the inerter system applied in building structures [24]. Xie et al. [25, 26] put forward a cable-bracing inerter system (CBIS), which is composed of cable and inerter energy dissipation system fixed at the bottom of interlayer of structure. And the study shows that it is easy to install and can effectively control structural displacement. Wang et al. [27] put forward a new tuned inerter-negative-stiffness damper (TINSD) for seismic protection of structures, which is more effective than the TID, TVMD, and INSD in reducing the dynamic response of structures.

In this study, a cable inerter viscous damper (CIVD) system is proposed. The end of the lightweight inerter viscous damper is directly connected with the elastic cable, which can be quickly installed in various plane and space structures. The system can not only realize structural reinforcement and improve the integrity of the structure but also realize the lightweight of the shock absorber. Firstly, Section 2 introduces the basic principle of IVD. By installing cables, the translation of the original structure is transformed into the rotation of IVD and the equivalent mass and equivalent damping of the shock absorber are improved. Then, in Section 3, the motion control equations and frequency response functions of the structure with CIVD are established. In Section 4, the parameter analysis is carried out to obtain the minimum inertia mass ratio and additional damping ratio of CIVD under different vibration mitigation standards. Finally, it carries out that the dynamic time history analysis of the structure installed with CIVD under the action of earthquake and fluctuating wind load in Section 5, verifies the vibration control effect of CIVD, and explains the vibration mitigation mechanism and the action of each element of CIVD in detail from the aspects of vibration mitigation rate and energy dissipation. The research in this study can provide a reference for the design of efficient and lightweight vibration mitigation scheme of plane and space structures based on the inerter damping system.

2. Theoretical Analysis of CIVD

2.1. Mechanical Model of Inerter Unit and CIVD. Compared with the mass unit, the inertia unit can increase the inertia by rotating. The two ends of the unit have different accelerations, and its output is also directly proportional to the relative acceleration at both ends, which can be expressed as follows:

$$f_I = m_d(a_2 - a_1), \tag{1}$$

where f_I is the output force of the inerter unit and a_1 and a_2 are the accelerations at both ends, and Figure 1 shows the mechanical model of the inerter element.

The inerter unit is the same as the mass unit and cannot dissipate energy by itself. It is generally used in combination with the damper. Figure 2(a) shows the inerter viscous damper (IVD), and the translation (Δ)can be converted into rotation (ϕ) in the damper through the ball screw. The mass in the damper generates kinetic energy through rotation, and the input energy can be dissipated by the viscous fluid in the damper. The

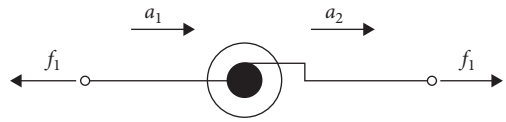

Figure 1: Mechanical model of an inerter element.

mechanical model of IVD is shown in Figure 2(b).Here, m_d and c_d are equivalent mass and equivalent damping coefficient, corresponding to the translation Δ at both ends of IVD; J and c_{vd} are the moment of inertia and viscous damping constants, corresponding to the rotation ϕ inside the IVD. The expressions of m_d and c_d can be obtained, where L is the lead of the ball screw:

$$m_d = \frac{4\pi^2}{L^2} J,$$
$$c_d = \frac{4\pi^2}{L^2} c_{vd}, \tag{2}$$
$$\phi = \frac{2\pi}{L} \Delta.$$

Cable inerter viscous damper (CIVD) is an elastic cable device added at the end of viscous inerter damper. Its mechanical model is basically consistent with tuned viscous mass damper (TVMD), and it is composed of series stiffness elements based on IVD. The mechanical model of CIVD is shown in Figure 3, and k_d is the equivalent stiffness of the cable device.

2.2. Mechanical Model of Single-Degree-of-Freedom (SDOF) System with CIVD. For a single-degree-of-freedom (SDOF) system, if only the installation of IVD is considered, the optimal value of the installation of IVD can be directly selected without considering the installation of angle (translation Δ of IVD is the same as the translation u of the single-degree-of-freedom system). The layout and mechanical model of the single-degree-of-freedom system installed with IVD are shown in Figure 4, where m, k and c are the mass, stiffness, and damping coefficients of the single-degree-of-freedom system respectively.

When considering layout of CIVD, the layout angle θ shall be considered. The layout efficiency β can be introduced, $\beta = \cos^2\theta$. After CIVD is installed, the equivalent stiffness k_d, equivalent damping coefficient c_d, and equivalent mass m_d shall be multiplied by the installation of efficiency β, becoming βk_d, βc_d, and βm_d. The single-degree-of-freedom system with layout of CIVD and mechanical model is shown in Figure 5.

2.3. Motion Control Equation and Frequency Response Function of SDOF with CIVD. If only the installation of IVD is considered, there is no relative displacement between SDOF and IVD because the IVD has no stiffness element ($\Delta = u$ and $\beta = 1$). According to the internal deformation coordination conditions of IVD provided by equation (2), it can be seen that the motion equation and dimensionless form of single-degree-of-freedom system with IVD under the action of vibration load $F_v(t)$ are as follows:

$$\begin{aligned} &m\ddot{u}'(t) + c\dot{u}'(t) + ku'(t) + m_d\ddot{u}'(t) + c_d\dot{u}'(t) \\ &= F_v(t), \left(1+\mu_d\right)\ddot{u}'(t) + 2\left(\zeta+\zeta_d\right)\omega_0\dot{u}'(t) + \omega_0^2 u'(t) \\ &= f_v(t), \end{aligned} \tag{3}$$

where $u\prime(t)$ is the displacement response of SDOF with IVD installed, μ_d and ζ_d are inertia mass ratio and additional viscous damping ratio respectively, κ_d is the additional stiffness ratio, ζ and ω_0 are the damping ratio and circular frequency of the original structure respectively, and $f_v(t)$ is the equivalent vibration load. If it is seismic action, $-f_v(t)$ is the acceleration of ground motion, and the expression of each parameter is as follows:

$$\zeta = \frac{c}{2m\omega},$$
$$\omega_0 = \sqrt{\frac{k}{m}},$$
$$f_v(t) = \frac{F_v(t)}{m},$$
$$\mu_d = \frac{m_d}{m}, \tag{4}$$
$$\zeta_d = \frac{c_d}{2m\omega_0},$$
$$\kappa_d = \frac{k_d}{k}.$$

On considering the stiffness of cable , the relative displacement will occur between SDOF and IVD ($\Delta \neq u$ and $0 < \beta < 1$). So CIVD generates additional degrees of freedom. $u(t)$ and $u_d(t)$ are the displacement responses of SDOF and CIVD respectively, and the following equation represents the motion control equation of SDOF with CIVD installed:

$$\begin{cases} m\ddot{u}(t) + c\dot{u}(t) + ku(t) + k_d\left(u(t)\cos\theta - u_d(t)\right)\cos\theta = F_v(t), \\ \beta m_d\ddot{u}_d(t) + \beta c_d\dot{u}_d(t) = k_d\left(u(t)\cos\theta - u_d(t)\right)\cos\theta. \end{cases} \tag{5}$$

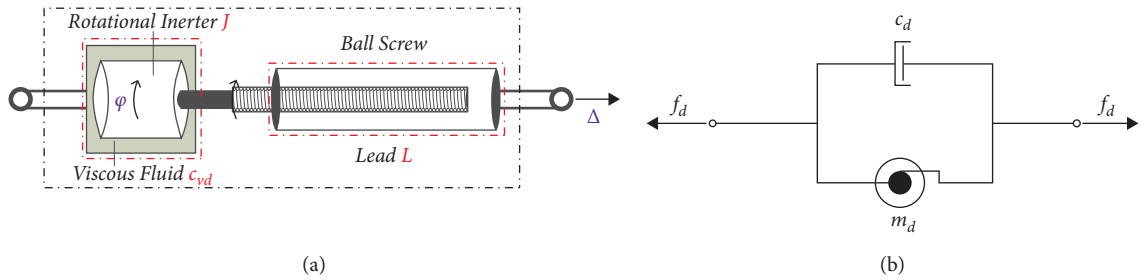

Figure 2: Structure and mechanical model of an inerter viscous damper (IVD): (a) IVD; (b) mechanical model.

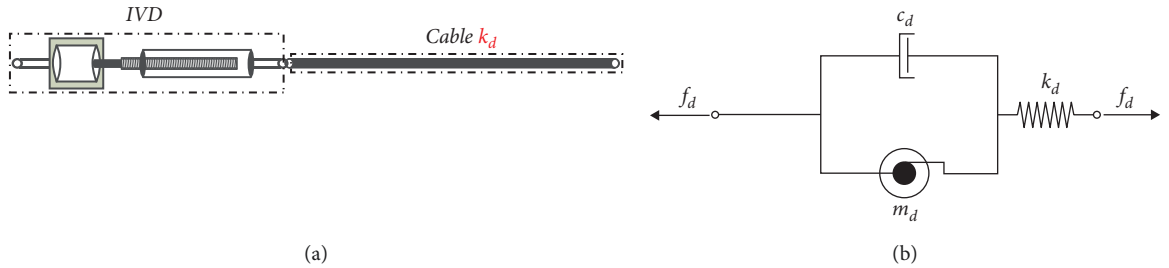

Figure 3: Mechanical model of a cable inerter viscous damper (CIVD): (a) CIVD; (b) mechanical model.

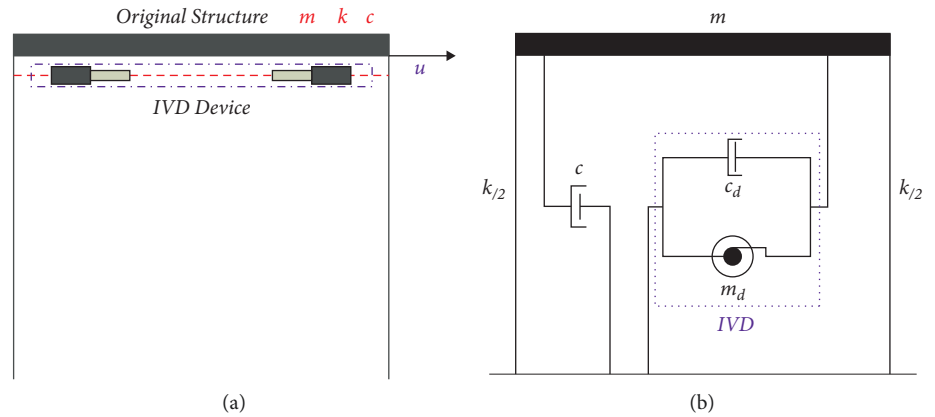

Figure 4: Layout and mechanical model of a SDOF with inerter viscous damper: (a) layout; (b) mechanical model.

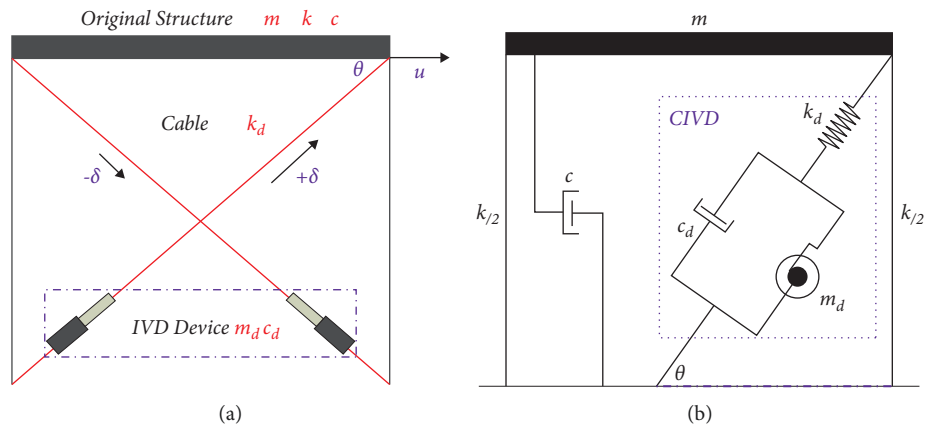

Figure 5: Layout and mechanical model of a SDOF with cable inerter viscous damper: (a) layout; (b) mechanical model.

Rewriting equation (5) into dimensionless form, the following equation can be obtained:

$$\begin{aligned}\left\{\ddot{u}(t)+2\zeta\omega_0\dot{u}(t)+(1+\beta\kappa_d)\omega u(t)-\kappa_d\cos\theta\omega_0^2u_d(t)=f_v(t),\beta\mu_d\ddot{u}_d(t)+2\beta\zeta_d\omega_0\dot{u}_d(t)\right.\\ \left.=(1+\beta\kappa_d)\omega_0^2u(t)-\kappa_d\cos\theta\omega_0^2u_d(t).\right.\end{aligned}\tag{6}$$

Laplace transform of equation (5) can be obtained:

$$\begin{cases}s^2U(s)+2\zeta\omega_0sU(s)+(1+\beta\kappa_d)\omega_0^2U(s)-\kappa_d\cos\theta\omega_0^2U_d(s)=F(s),\\ \beta\mu_ds^2U_d(s)+2\beta\zeta_d\omega_0sU_d(s)=(1+\beta\kappa_d)\omega_0^2U(s)-\kappa_d\cos\theta\omega_0^2U_d(s),\end{cases}\tag{7}$$

where $S=i\Omega$, Ω is the excitation frequency of vibrational load, and $U(s)$, $U_d(s)$, and $F(s)$ are the Laplace transform of $u(t)$, $u_d(t)$, and $f_v(t)$ respectively. From equation (7), $U(s)$ and $U_d(s)$ can be solved as follows:

$$\begin{cases}U(s)=\dfrac{\left(\beta\mu_ds^2+2\beta\mu_ds\omega_0+\kappa_d\cos\theta\omega_0^2\right)F(s)}{D(s,\beta,\zeta,\mu_d,\zeta_d,\kappa_d,\omega_0)},\\ U_d(s)=\dfrac{\beta\kappa_d\omega_0^2F(s)}{D(s,\beta,\zeta,\mu_d,\zeta_d,\kappa_d,\omega_0)},\end{cases}\tag{8}$$

where

$$\begin{aligned}D(s,\beta,\zeta,\mu_d,\zeta_d,\kappa_d,\omega_0)=s^4\beta\mu_d+s^3(2\beta\zeta_d+2\beta\zeta\mu_d)\omega_0+s^2\left(\kappa_d\cos\theta+\beta\mu_d+4\beta\zeta\zeta_d+\beta^2\kappa_d\mu_d\right)\omega_0^2\\ +s\left(2\beta\zeta_d+2\beta^2\kappa_d\zeta_d+2\kappa_d\zeta\cos\theta\right)\omega_0^3+(1+\beta\mu_d)\kappa_d\cos\theta\omega_0^4.\end{aligned}\tag{9}$$

Then, the SDOF displacement response transfer function $H_U(s)$ of the installation of CIVD and the force response transfer function $H_d(s)$ of the CIVD can be obtained from equations (7)–(9):

$$\begin{cases}H_U(s)=\dfrac{U(s)}{F(s)},\\ H_d(s)=\dfrac{U_d(s)}{F(s)}\left(\beta\mu_ds^2+2\beta\zeta_d\omega_0s\right).\end{cases}\tag{10}$$

3. Parameter Analysis of CIVD System

According to Parseval's theorem, the root mean square response of the system σ excited by white noise is obtained as follows:

$$\begin{aligned}\sigma&=\int_0^T\frac{u^2(t)}{T_0}\mathrm{d}t\\ &=\sqrt{\int_{-\infty}^{+\infty}|H(i\Omega)|^2S_0\mathrm{d}\Omega},\end{aligned}\tag{11}$$

where S_0 is the white noise power spectrum. In modern control theory, the root mean square response (RMS) of linear system σcan be referred to as H_2 norm, and the relative frequency α is introduced. Then, the root mean square response can be rewritten as follows:

$$\sqrt{\int_{-\infty}^{+\infty}|H(i\alpha\omega)|^2}=\|H(i\alpha\omega)\|_2,\quad \alpha=\frac{\Omega}{\omega}.\tag{12}$$

Therefore, the effect of the shock absorber can be measured by comparing the reduction rate of the displacement root mean square response of the original system before and after vibration mitigation. For SDOF structure with CIVD installed, its mitigation ratio of displacement response η_U is as follows:

$$\begin{aligned}\eta_U&=\frac{\sigma_U}{\sigma_{U_0}}\\ &=\frac{\left\|H_U(i\alpha\omega)\right\|_2}{\left\|H_{U_0}(i\alpha\omega)\right\|_2}.\end{aligned}\tag{13}$$

where σ_{U0} is the displacement root mean square response of the original structure (SDOF) and H_{U0} is the displacement transfer function of the original structure; σ_U is the displacement root mean square response of SDOF installed with CIVD. The clearer the mitigation ratio of displacement response is, the better the effect of the shock absorber is.

Parameter analysis include inertia mass ratio μ_d, additional viscous damping ratio ζ_d, and additional stiffness ratio κ_d. The natural damping ratio ζ of the original structure (SDOF) is assumed to be 0.02. The mitigation ratio of displacement response η_U of SDOF due to the installation of CIVD is related to all three parameters, which is difficult to see directly changes of η_U with the joint change of the three parameters. Therefore, one should be fixed and the changes of the other two parameters should be observed. The parameter range of inertia mass ratio μ_d during parameter analysis and additional viscous damping ratio ζ_d are [0.01,1] and the parameter range of the stiffness ratio κ_d is [0.01,10]. In addition, due to the layout angle of the cable θ and layout efficiency β, it has a great impact on the performance of CIVD, which should also be considered in the analysis. Therefore, in the following analysis, the layout angle $\theta = 45^\circ$ and layout efficiency $\beta = 0.5$ are considered.

3.1. Stiffness Ratio κ_d. Firstly, the values of κ_d are set as 0.01, 0.02, 0.05, 0.1, 0.2, 0.5, 1, 2, 5, and 10, respectively, and the variation diagram of η_U with $\mu_d - \zeta_d$ two-dimensional space can be seen with variation of κ_d. Figure 6 shows the variation trend of η_U with different stiffness ratios κ_d under $\mu_d - \zeta_d$ two-dimensional space. If the target mitigation ratio of displacement response is determined to be 50%, it can be seen that when $\kappa_d > 0.5$, the area enclosed by the target isopleth of η_U is larger, and when $\kappa_d > 1$, the area enclosed by the isopleth of η_U is basically stable, then the value range of κ_d is determined to be between 0.5 and 1, and η_U with $\mu_d - \zeta_d$ is made at the same time, considering $\kappa_d = 0.5$ and $\kappa_d = 1$.

It can be seen by comparing Figures 6(b) and 6(c), the damping effect is similar under $\kappa_d = 0.5$ and $\kappa_d = 1$, the minimum mitigation ratio of displacement response is about 0.5, the best range of μ_d is 0.2–0.5, and the minimum value of ζ_d is about 0.1. By comparing with the displacement amplification factor of the original structure, it can be seen that the vibration mitigation effect of CIVD is significant and the reduction range of the maximum response is between 70% and 85%, as shown in Figure 7(c). However, compared with Figures 7(a) and 7(b), when $\kappa_d = 0.5$ and additional damping ratio ζ_d increases between 0.4 and 1, the response of the main structure also increases. Although the increase is only about 10%, this is not allowed in practical engineering. Because the additional damping ratio will increase the cost of engineering project. So from the fixed value of the stiffness ratio κ_d, we can determine the optimal value range of $\mu_d - \zeta_d$, but each parameter cannot be obtained in two-dimensional space. To this end, we should continue to analyze $\mu_d - \zeta_d$ and the two-dimensional space variation law of other parameter combinations.

Due to the mass and damping amplification effect of IVD, the effect is higher than the original several times with small mass and small damping coefficient, so as to realize the lightweight of the damper. Therefore, the target mitigation ratio of response of the original structure should be guaranteed while reducing as much as possible μ_d and ζ_d. It is also the basic principle of parameter optimization.

3.2. Inertia-Mass Ratio μ_d. Then the parameters μ_d.will be fixed. The fixed values of μ_d are 0.01, 0.02, 0.05, 0.1, 0.2, 0.5, and 1, respectively, and the variation diagram of η_U under $\kappa_d - \zeta_d$ two-dimensional space can be seen. Figure 8 shows the variation trend of η_U with different inertia mass ratio μ_d under $\kappa_d - \zeta_d$ two-dimensional space. If the target mitigation ratio of displacement response is determined to be 50%, it can be seen that when μ_d is in the range of 0.05–0.2, the area enclosed by the target isopleth of η_U is larger and the area enclosed by the isopleth increases firstly and then decreases, and when μ_d is in the range of 0.01–0.05, the change of η_U is small, so it can be determined that the value of μ_d is between 0.05 and 0.2 and η_U under $\kappa_d - \zeta_d$ two-dimensional space is made under $\mu_d = 0.05$, $\mu_d = 0.1$, and $\mu_d = 0.2$.

It can be seen by comparing Figures 8(b) and 8(c), the maximum mitigation ratio of displacement response is the same under $\mu_d = 0.05$, $\mu_d = 0.1$, and $\mu_d = 0.2$, when $\eta_U = 50\%$ under the same damping ratio; the max requirement of additional damping ratio is $\mu_d = 0.2$ and $\mu_d = 0.05$ and the min requirement of additional damping ratio is $\mu_d = 0.1$. Although when $\mu_d = 0.2$, the area enclosed by the blue damping ratio contour is larger, but the additional damping ratio ζ_d mostly needs more than $\mu_d = 0.05$, which also violates the principle of damping amplification through CIVD system. The value of inertia mass ratio near $\mu_d = 0.2$ should be discarded, and $\mu_d = 0.05 - 0.1$. Figure 8(e) shows the displacement amplification factor of the original structure. Under the same damping ratio, the values of $\mu_d = 0.05$ and $\mu_d = 0.1$ are almost the same, all less than the value under $\mu_d = 0.2$.

3.3. Additional Damping Ratio ζ_d. Finally, the parameters $\zeta_d$will be fixed.The fixed values of ζ_d are 0.01, 0.02, 0.05, 0.1, 0.2, 0.5, and 1, respectively, and the variation diagram of η_U under $\kappa_d - \mu_d$ two-dimensional space can be seen. Figure 9 shows the variation trend of η_U with different additional damping ratio μ_d under $\kappa_d - \mu_d$ two-dimensional space. Similarly, if the target mitigation ratio of displacement response is determined to be 50%, it can be realized when $\zeta_d > 0.05$. η_U is basically stable within the range of 0.2–1 of the additional damping ratio, so we can fix the value range of additional damping ratio to be between 0.05 and 0.2, and η_U under $\kappa_d - \mu_d$ two-dimensional space is made under $\zeta_d = 0.05$, $\zeta_d = 0.1$, and $\zeta_d = 0.2$.

Although the maximum mitigation ratio of displacement response under the value of $\zeta_d = 0.05$ and $\zeta_d = 0.1$ is less than the value of $\zeta_d = 0.2$, the value of ζ_d is in the range of 0.05–0.1. The blue vibration mitigation of η_U is larger than the area enclosed by contour lines, indicating that the value range of κ_d and $\mu_d$is greater. And the

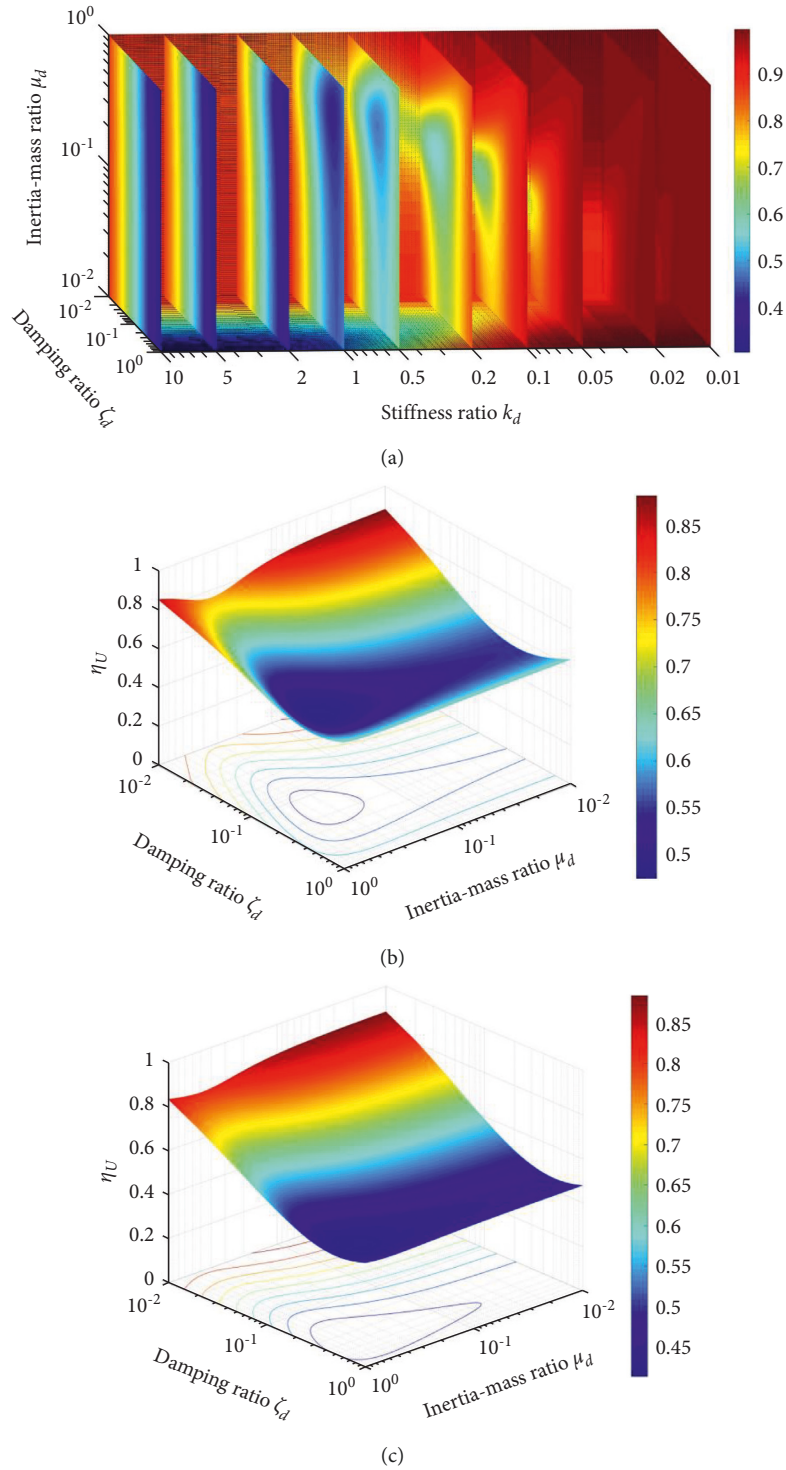

Figure 6: Mitigation ratio of displacement response: (a) changing κ_d; (b) $\kappa_d = 0.5$; (c) $\kappa_d = 1$.

smaller value of $\mu_d$meets lightweight requirements of CIVD's design. If $\eta_U = 0.6$ is the target mitigation ratio of design, then the inertia mass ratio is comprehensively controlled. The value, near $\zeta_d = 0.05$, is the optimal design value. But if $\eta_U = 0.6$ is the target mitigation ratio of design, then the value near $\zeta_d = 0.1$ is the optimal design value. The smaller the mitigation ratio of displacement response is, the better the performance of the IVD shock absorber is, but the more rigorous the selection of parameters is, and the smaller the value range of the optimal parameters is. So the minimum additional damping ratio ζ_d shall be analyzed according to the needs of the project.

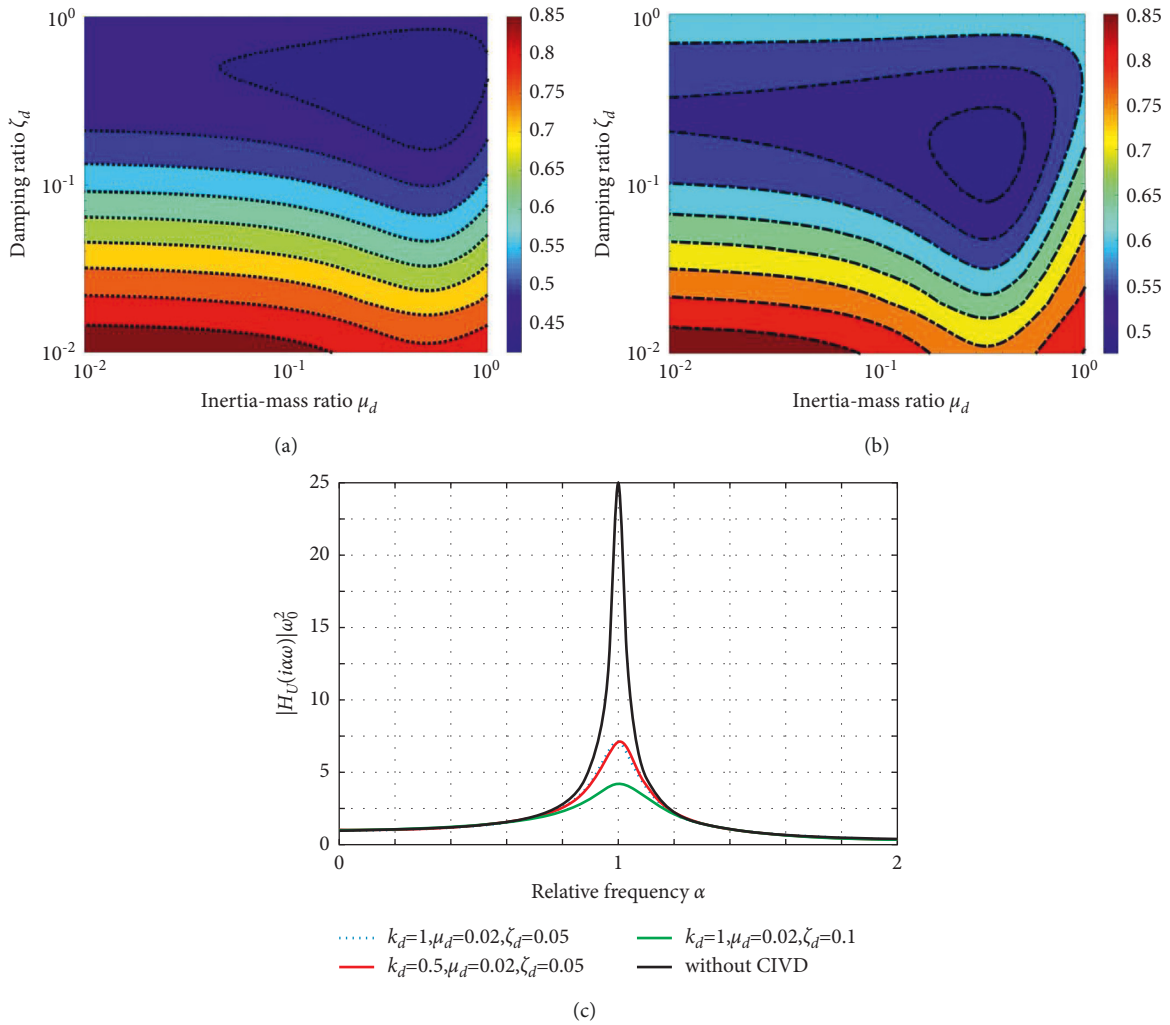

Figure 7: Isopleth of mitigation ratio of displacement response: (a) $\kappa_d = 0.5$; (b) $\kappa_d = 1$; (c) displacement amplification factor.

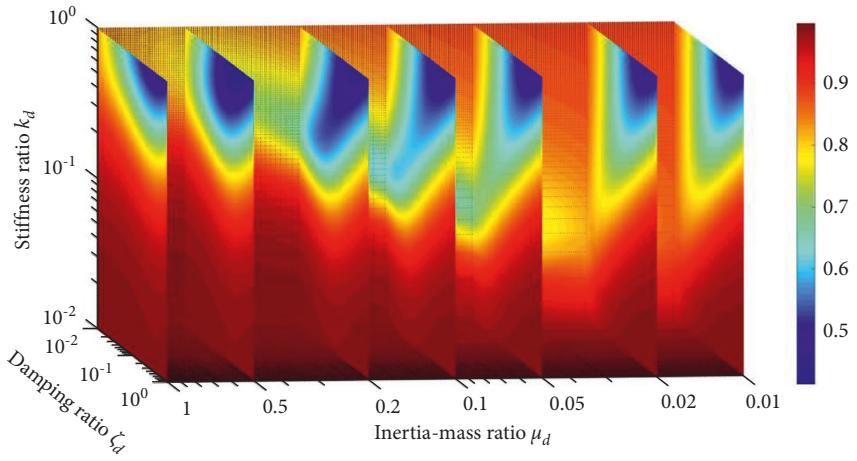

Figure 8: Continued.

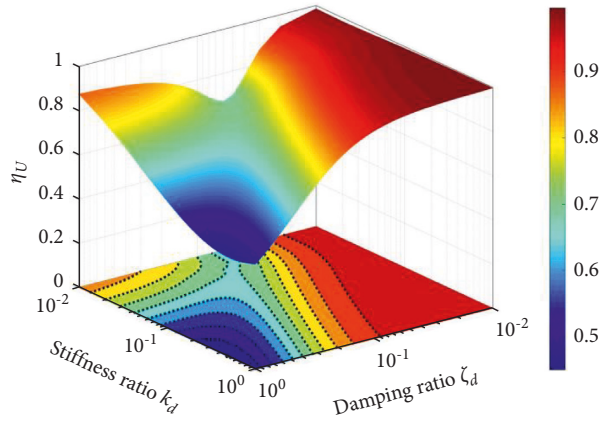

(b)

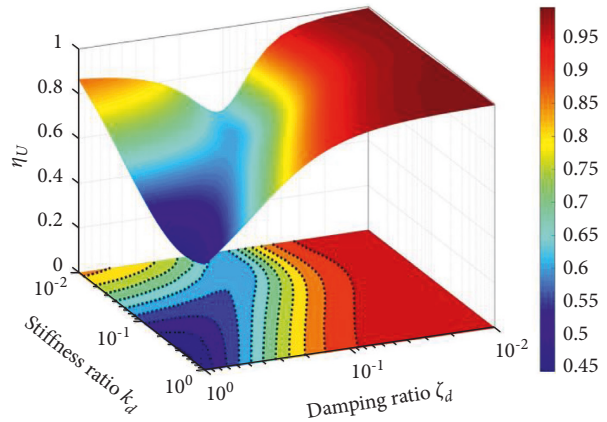

(c)

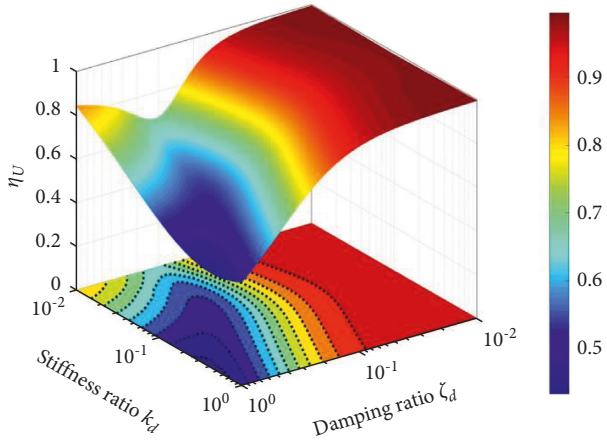

(d)

FIGURE 8: Continued.

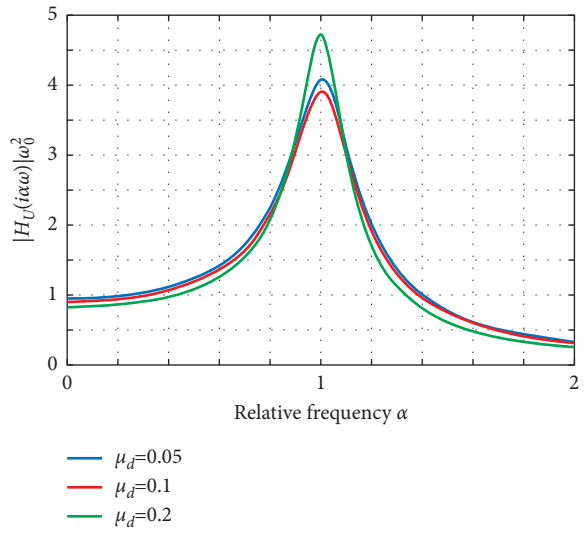

(e)

Figure 8: Mitigation ratio of displacement response: (a) changing μ_d; (b) $\mu_d = 0.05$; (c) $\mu_d = 0.1$; (d) $\mu_d = 0.2$; (e) displacement amplification factor ($\kappa_d = 1$, $\zeta_d = 0.1$).

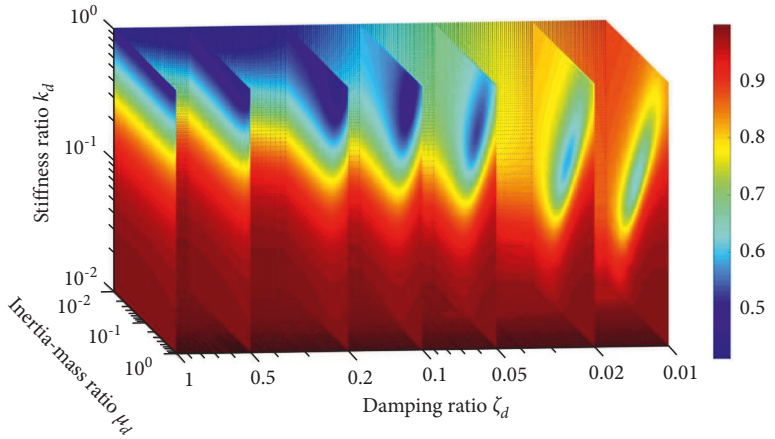

(a)

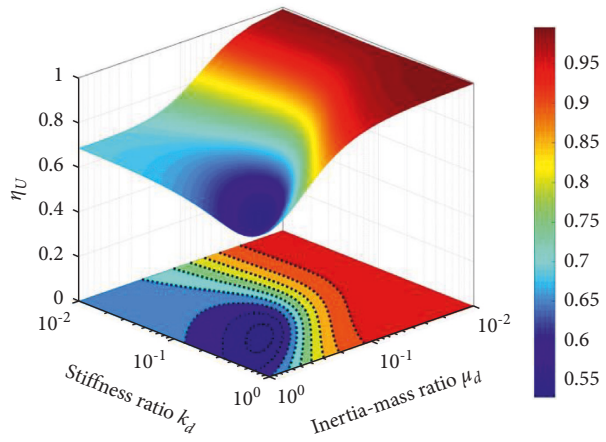

(b)

Figure 9: Continued.

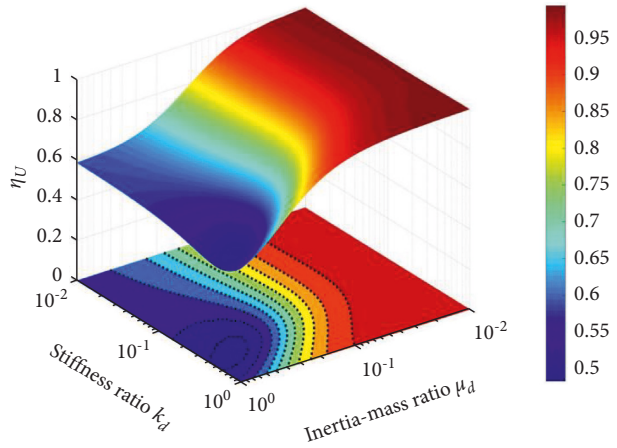

(c)

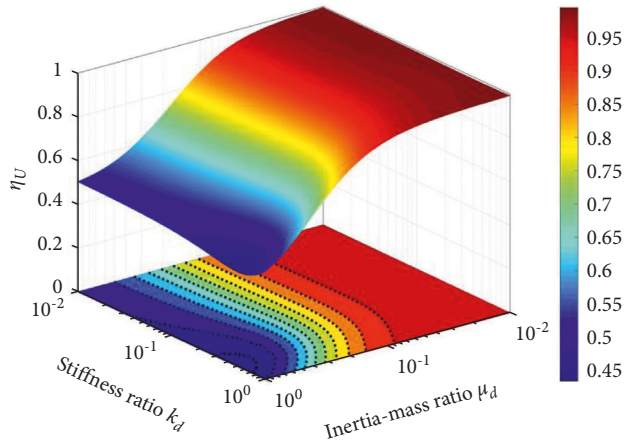

(d)

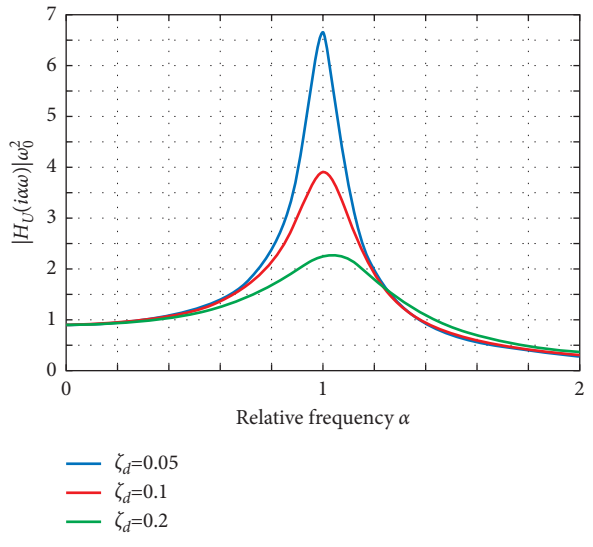

(e)

FIGURE 9: Mitigation ratio of displacement response: (a) changing ζ_d; (b) $\zeta_d = 0.05$; (c) $\zeta_d = 0.1$; (d) $\zeta_d = 0.2$; (e) displacement amplification factor ($\kappa_d = 1$, $\zeta_d = 0.1$).

Figure 9(e) shows the displacement amplification factor of the original structure, which can be seen that ζ_d can obviously alleviate the resonance response of the original structure and increase the frequency response bandwidth.

3.4. Optimal Design of the CIVD. The selection of design parameters of CIVD or other inerter dampers can be determined by the fixed-point method [28]. Based on the fixed-point theory, Ikago et al. [15]proposed design methods for single-degree-of-freedom structure and multi-degree-of-freedom structure installed with inerter dampers respectively. For the single degree of freedom system with CIVD, after the μ_d is determined, if the layout angle θ of the cable is not considered, the stiffness ratio and damping ratio can be obtained by the following equation:

$$\begin{aligned} \kappa_d &= \frac{\mu_d}{1-\mu_d}, \\ \zeta_d &= \frac{\mu_d}{2}\sqrt{\frac{3\mu_d}{(1-\mu_d)(2-\mu_d)}}. \end{aligned} \tag{14}$$

However, the fixed-point theory does not consider the natural damping of the main structure and external excitation characteristics and cannot consider other performance requirements of the main structure. For example, in this study, the key control indexes such as the displacement response of SDOF cannot be reflected. Therefore, when designing parameters of CIVD, we should consider the main performance of the main structure, firstly, such as determining the target mitigation ratio of displacement response η_U according to the structural performance requirements and optimizing the parameters with extremum conditions [16, 29], that is:

$$\eta_U(\zeta_d, \kappa_d, \mu_d) = \eta_{U,t}, \tag{15}$$

$$\begin{aligned} \frac{\partial \eta_U(\zeta_d, \kappa_d, \mu_d)}{\partial \mu_d} &= 0, \\ \frac{\partial \eta_U(\zeta_d, \kappa_d, \mu_d)}{\partial \zeta_d} &= 0, \end{aligned} \tag{16}$$

where $\eta_{U,t}$ is the target mitigation ratio of displacement response. The larger the damping ratio and inertia-mass ratio, the more difficult it is to achieve in the installation of CIVD in engineering. So the mathematical problem shows in equation (15) and equation (16): for a given κ_d is equal to the extremum condition that the partial derivative of η_U with respect to μ_d and ζ_d are set as zero. Therefore, the constraint condition of equation (16) is to meet the target mitigation ratio of displacement response $\eta_{U,t}$. At the same time, the damping ratio and inertia-mass ratio are made as small as possible to meet the engineering needs.

4. Dynamic Response Analysis of CIVD System

In order to verify the vibration mitigation effect of CIVD, making $\eta_U = 0.5$ as the target mitigation ratio of displacement response, optimal parameters are taken as $\mu_d = 0.13$, $\zeta_d = 0.11$, and $\kappa_d = 1.0$. The reason for the selection of large stiffness ratio of the cable is to prevent the prestress relaxation of the cable from reducing the nonlinear stiffness of the cable. If the stiffness of cable is nonlinear, the results of analytical stochastic response in this study will be inaccurate and the parameter design method of CIVD will be inapplicable. Therefore, the layout angle of the cable should be small as much as possible to avoid the application of CIVD in long-span structures.

We carry out the dynamic response analysis of the single degree of freedom system with CIVD installed under seismic waves and fluctuating wind load input. Figure 10 shows the corresponding displacement amplification factor of the original structure. The original structural mass $m = 2.1 \times 10^4$kg, stiffness $k = 1.5 \times 10^4$N/m, inherent damping ratio $\zeta = 0.02$, moment of inertia J of inerter viscous damper is $0.007\text{kg} \cdot \text{m}^2$, viscous damping constant is $0.09\text{N} \cdot \text{m} \cdot \text{s}$, and ball screw lead $L = 0.01m$.

El Centro wave, Taft wave, Chi Chi wave and Kobe wave are selected as seismic waves, the peak ground acceleration (PGA) is adjusted to 0.4 g, the davenport spectrum is selected as fluctuating wind spectrum, and the wind speed $v_{10} = 40m/s$, v_{10} is the average wind speed at 10 m. Figure 11 shows the response spectrum of four seismic waves and the power spectrum density of fluctuating wind.

Figure 12 shows the displacement time history response of the original structure. It can be seen that CIVD has good vibration damping performance. At the same time, the peak value and root mean square value of displacement response are selected to evaluate the vibration damping performance of CIVD. The peak value reflects the maximum dynamic response at a certain time, while the root mean square value reflects the overall energy of the whole time history of the structure, that is, the power spectrum corresponding to the dynamic response of the whole time history. Therefore, we define the displacement reduction coefficient to evaluate the vibration damping performance of CIVD, and reduction coefficients are shown in the following equation:

$$\begin{aligned} \lambda_p &= \frac{u_{0p} - u_{cp}}{u_{0p}}, \\ \lambda_r &= \frac{u_{0r} - u_{cr}}{u_{0r}}, \end{aligned} \tag{17}$$

where λ_p and λ_r are reduction coefficients of displacement peak value and root mean square value respectively, u_{0p} and u_{cp} are displacement peak values of original structure and CIVD installed structure respectively, u_{0r} and u_{cr} are displacement root mean square values of original structure and CIVD installed structure respectively. Table.1 lists the peak displacement and root mean square reduction coefficient of CIVD system under the action of four seismic waves and fluctuating wind. It can be seen from Figure 12 and Table 1 that the vibration of SDOF system with CIVD is effectively controlled. The peak

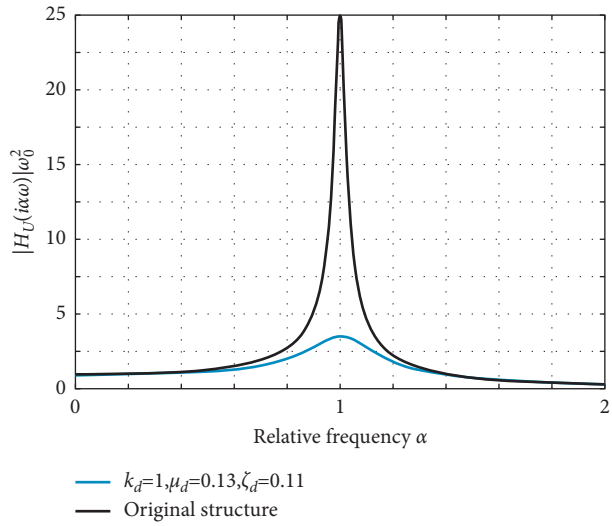

Figure 10: Displacement amplification factor ($\kappa_d = 1$, $\mu_d = 0.1$, $\zeta_d = 0.11$, $\zeta = 0.02$).

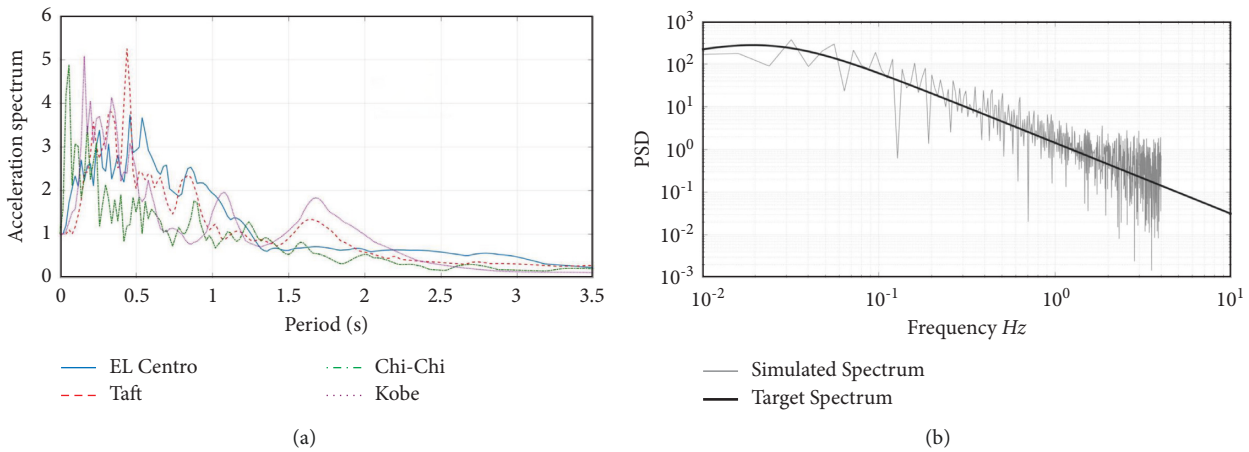

Figure 11: Normalized acceleration spectra of earthquake records and davenport spectrum of fluctuating wind.

displacement control effect is 30%–50%, and the root mean square displacement control effect is 40%–70%. CIVD has a good effect on the continuous vibration control of the original structure, and the controlled structural displacement can quickly enter the stable state of small displacement.

Figure 13 shows the comparison of damping force and displacement of main structure (u) curves between SDOF system with CIVD and the original structure. Under five input conditions, it shows good energy dissipation capacity: large damper output and low displacement response of main structure.

Figure 14 compares the displacement damping effect of cable inerter damping system (CID) and cable inerter viscous damping system (CIVD), the revolutions per second (RPS) of inertia container and the output of inertial force and damping force of structural system. As can be seen from Figure 14(a), even if there is no damping device, the inerter element can obtain a certain vibration mitigating effect on the original structure through mass rotating amplification, so as to make the structure enter a stable state. However, since the inerter element has no energy dissipation effect, the vibration in a stable state cannot be attenuated rapidly. As can be seen from Figure 14(b), the speed per second of CID is much higher than that of CIVD, and the average speed in the whole time range is 2.29 times that of CIVD. It also shows that the horizontal shaking speed of the original structure with CID is higher than that of CIVD, and long-term high-speed rotation will reduce the service life of the inerter element. Therefore, additional damping is needed to restrain the translation of the main structure and the rotation of the inerter element. Figure 14(b) compares the sum of the total inertial force and damping force of the original structure, SDOF system with CID installed and SDOF system with CIVD installed.

It can be seen that the inertial force of the original structure can be greatly reduced, and the additional damping can improve the energy dissipation effect, reduce the displacement, make the additional damping force dominant, and suppress the structural vibration effectively.

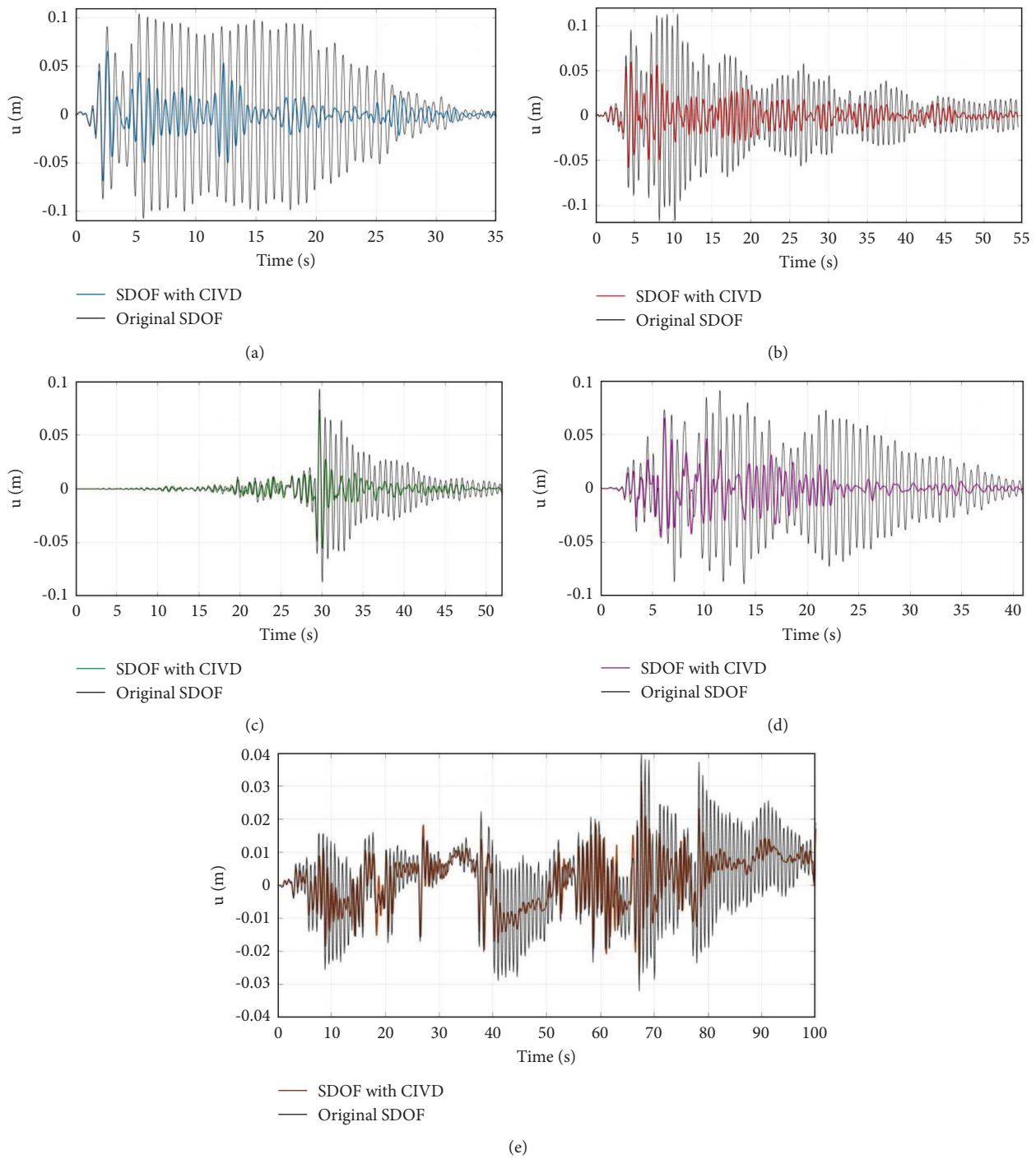

Figure 12: Displacement response (u) time histories of SDOF with and without CIVD under:(a) the El Centro record; (b) the Taft record; (c) the Chi-Chi record; (d) the Kobe record; (e) fluctuating wind.

Figure 15 shows the comparison of the displacement and damping force of the damper when TMD and CIVD are installed in the main structure under the same target mitigation ratio of displacement response ($\eta_U = 0.5$). The optimal design method of TMD is the same as that of CIVD. It can be seen that the deformation of the damping element in CIVD is significantly greater than that in TMD due to the existence of inerter system. Although the damping forces of CIVD and TMD are almost the same, due to the large deformation of the damping element, CIVD can provide a satisfactory effect of energy dissipation.

Compared with TMD, CIVD does not improve the damping effect by increasing the damping coefficient in the damping device directly but increases the equivalent damping through rotating amplification. With a small moment of inertia and damping constant, the additional inertia mass ratio and damping ratio of CIVD under the target damping ratio can be achieved, making shock

Table 1: λ_p and λ_r of original structure under earthquake and fluctuating wind.

Input	El centro	Taft	Chi-chi	Kobe	Fluctuating wind
λ_p (%)	36.10	49.32	30.86	38.18	36.99
λ_r (%)	69.12	62.17	51.90	61.61	40.72

absorber smaller, and it makes up for the defects of traditional TMD due to its large volume and big mass in

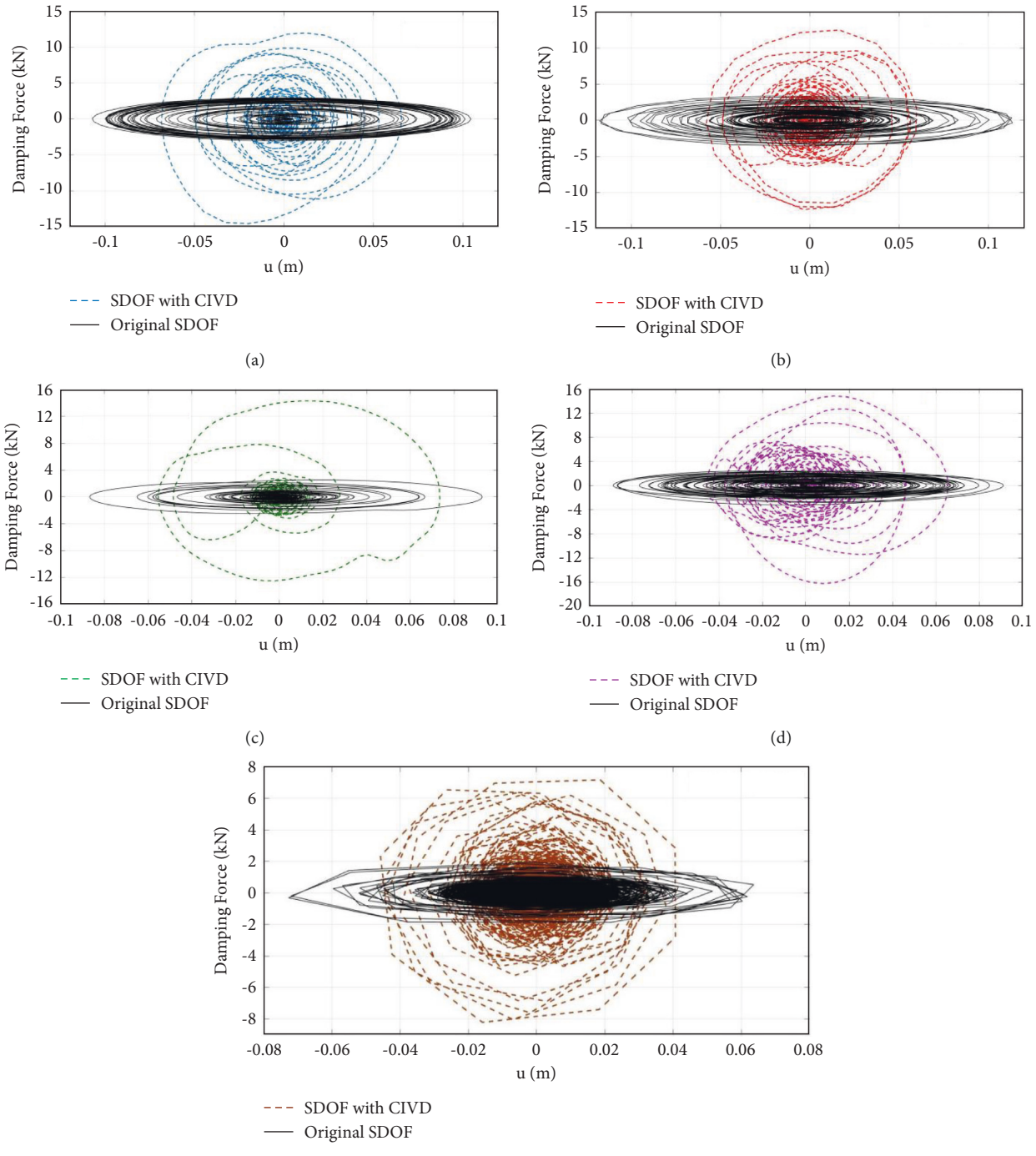

Figure 13: Damping force and displacement of main structure (u) curves of SDOF with and without CIVD under: (a) the El Centro record; (b) the Taft record; (c) the Chi-Chi record; (d) the Kobe record; (e) fluctuating wind.

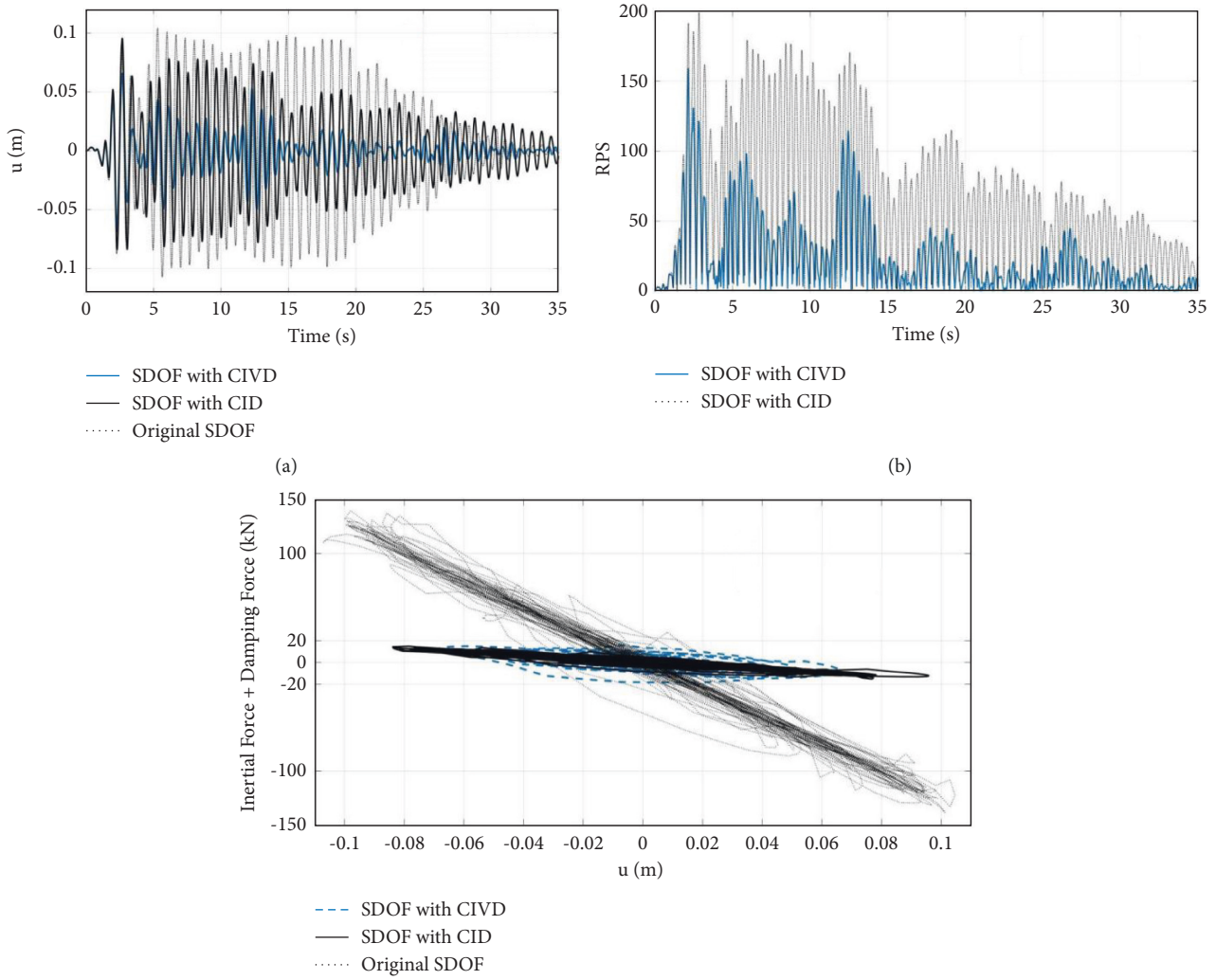

Figure 14: Response of SDOF with CIVD and CID under El Centro wave: (a) time history; (b) RPS of the inerter element; (c) hysteretic curves of the inertial force and damping force.

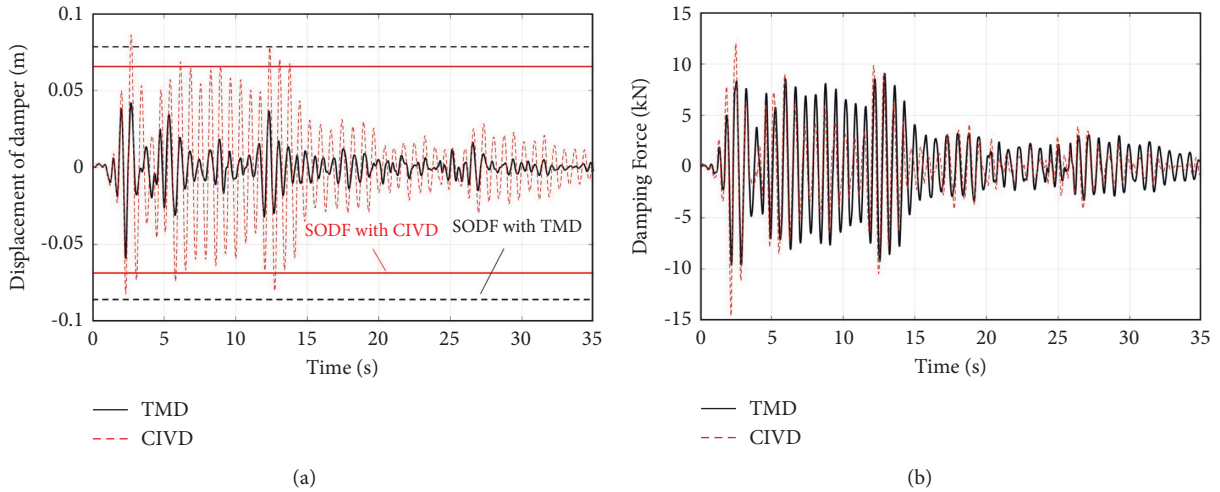

Figure 15: Response of damping element of CIVD and TMD under El Centro wave: (a) displacement; (b) damping force.

practical engineering.

5. Conclusions

Firstly, this study introduces the mechanical model of the cable inerter viscous damping system (CIVD) and establishes the vibration control equation of the single degree of freedom system (SDOF) with CIVD installed. Then, the parameter of inertia mass ratio, additional damping ratio, and stiffness ratio are studied. Finally, the dynamic time history analysis of the SDOF with CIVD installed under seismic action and fluctuating wind load is carried out. The performance of vibration mitigation of CIVD is verified. The main conclusions are as follows:

(1) The cable inerter viscous damping system (CIVD) can enlarge the mass and damping through rotation, realize the lightweight and high efficiency of the damper, and make up for the defects of the traditional TMD system in engineering. When designing CIVD, the inertia mass ratio and additional damping ratio should be reduced as much as possible under the condition of meeting the target damping ratio.

(2) CIVD can significantly suppress the resonance response of the structure and make the continuous vibration response into a stable state. The peak displacement can be reduced by 30%–50%, and the root mean square displacement can be reduced by 40%–70%. At the same time, the energy dissipation capacity of the damping element is also greatly strengthened.

(3) Installing the cable and inerter element (CID) can only control the structural vibration, but it cannot reduce the amplitude in the steady state. The CID can control the inertial force output of the original structure, but the rotational speed of the inerter element is high and the shaking speed of the structure is fast. But we can control the acceleration, velocity, and displacement of the original structure at the same time, if we add the inertia, additional damping, and additional stiffness. Meanwhile, the deformation of the damping element in CIVD is enlarged compared with TMD under the same target mitigation ratio of displacement response.

In conclusion, the CIVD system has a good vibration mitigation effect. This study mainly focuses on the macrostructural design parameters, but there is no detailed analysis on the design parameters of specific cable inerter viscous damper. At present, the cable inerter viscous damping device is in the development stage. The subsequent research will carry out the mechanical performance test according to the specific inerter damping device. Furthermore, the shaking table test will be carried out on the specific structure with CIVD or IVD installed.

Data Availability

The method of this paper is mainly formula derivation, and the data can be obtained from this paper directly. If And the data of section 4 (dynamic analysis) can be obtained with the first author.

Conflicts of Interest

The authors declare that they have no conflicts of interest.

Acknowledgments

This research was supported by State Grid Science & Technology Project (5200–201919121A-0-0-00) and 2020 open fund project of the State Key Laboratory of Disaster Prevention & Reduction for Power Grid Transmission and Distribution Equipment (B316AF190007).

References

[1] M. Cao, F. Zhou, P. Tan, G. Zhang, Y. F. Cheng, and Z. B. Dai, "Seismic response of transformer and bushing isolation system and parameter analysis of isolation layer," *Journal Proceedings of the CSEE*, vol. 32, no. 13, pp. 166–174, 2012.

[2] L. Tian, H. Pan, and R. Ma, "Probabilistic seismic demand model and fragility analysis of transmission tower subjected to near-field ground motions," *Journal of Constructional Steel Research*, vol. 156, pp. 266–275, 2019.

[3] L. Meirovitch, *Dynamics and Control of Structures*, John Wiley & Sons, Hoboken, NJ, USA, 1990.

[4] T. T. Soong and G. F. Dargush, *Passive Energy Dissipation Systems in Structural Engineering*, Wiley, New York, NY, USA, 1997.

[5] G. W. Housner, L. A. Bergman, T. K. Caughey et al., "Structural control: past, present, and future," *Journal of Engineering Mechanics*, vol. 123, pp. 897–971, 1997.

[6] A. Kareem, T. Kijewski, and Y. Tamura, "Mitigation of motions of tall buildings with specific examples of recent applications," *Wind and Structures*, vol. 2, no. 3, pp. 201–251, 1999.

[7] R. J. McNamara, "Tuned mass dampers for buildings," *Journal of the Structural Division ASCE*, vol. 103, 1977.

[8] J.-S. Hwang, J. Kim, S.-H. Lee, and K.-W. Min, "Equivalent damping of a structure with vibration control devices subjected to wind loads," *Wind and Structures*, vol. 6, no. 4, pp. 249–262, 2003.

[9] E. Simiu and R. Scanlan, *Wind Effects on Structures*, Wiley, New York, NY, USA, 1996.

[10] L. Tian, H. Pan, C. Qiu, R.-S. Ma, and Q.-Q. Yu, "Wind-induced collapse analysis of long-span transmission tower-line system considering the member buckling effect," *Advances in Structural Engineering*, vol. 22, no. 1, pp. 30–41, 2019.

[11] S.-H. Lee, K.-W. Min, J.-S. Hwang, and J. Kim, "Evaluation of equivalent damping ratio of a structure with added dampers," *Engineering Structures*, vol. 26, no. 3, pp. 335–346, 2004.

[12] M. C. Smith and F.-C. Wang, "Performance benefits in passive vehicle suspensions employing inerters," *Vehicle System Dynamics*, vol. 42, no. 4, pp. 235–257, 2004.

[13] M. C. Smith, "Synthesis of mechanical networks: the inerter," *IEEE Transactions on Automatic Control*, vol. 47, no. 10, pp. 1648–1662, 2002.

[14] S. J. Swift, M. C. Smith, A. R. Glover, C. Papageorgiou, B. Gartner, and N. E. Houghton, "Design and modelling of a fluid inerter," *International Journal of Control*, vol. 86, no. 11, pp. 2035–2051, 2013.

[15] K. Ikago, K. Saito, and N. Inoue, "Seismic control of single-degree-of-freedom structure using tuned viscous mass damper," *Earthquake Engineering & Structural Dynamics*, vol. 41, no. 3, pp. 453–474, 2012.
[16] C. Pan and R. Zhang, "Design of structure with inerter system based on stochastic response mitigation ratio," *Structural Control and Health Monitoring*, vol. 25, no. 6, 2018.
[17] C. Pan, R. Zhang, H. Luo, C. Li, and H. Shen, "Demand-based optimal design of oscillator with parallel-layout viscous inerter damper," *Structural Control and Health Monitoring*, vol. 25, no. 1, 2018.
[18] J.-S. Hwang, J. Kim, and Y.-M. Kim, "Rotational inertia dampers with toggle bracing for vibration control of a building structure," *Engineering Structures*, vol. 29, no. 6, pp. 1201–1208, 2007.
[19] H. Luo, R. Zhang, and D. Weng, "Mitigation of liquid sloshing in storage tanks by using a hybrid control method," *Soil Dynamics and Earthquake Engineering*, vol. 90, pp. 183–195, 2016.
[20] R. Zhang, Z. Zhao, and K. Dai, "Seismic response mitigation of a wind turbine tower using a tuned parallel inerter mass system," *Engineering Structures*, vol. 180, pp. 29–39, 2019.
[21] Z. P. Zhao, R. F. Zhang, N. E. Wierschem, Y. Y. Jiang, and C. Pan, "Displacement mitigation-oriented design and mechanism for i," *Journal of Vibration and Control*, 2020.
[22] H. Gao, H. Wang, J. Li et al., "Optimum design of viscous inerter damper targeting multi-mode vibration mitigation of stay cables," *Engineering Structures*, vol. 226, Article ID 111375, 2021.
[23] Y. Sugimura, W. Goto, H. Tanizawa, K. Saito, and T. Nimomiya, "Response control effect of steel building structure using tuned viscous mass damper," in *Proceedings of the The 15th World Conference on Earthquake Engineering*, Lisbon, Portugal, September 2012.
[24] M. Kurata, R. T. Leon, and R. Desroches, "Rapid seismic rehabilitation strategy: concept and testing of cable bracing with couples resisting damper," *Journal of Structural Engineering*, vol. 138, no. 3, pp. 354–362, 2012.
[25] L. Xie, X. Ban, S. Xue, K. Ikago, J. Kang, and H. Tang, "Theoretical study on a cable-bracing inerter system for seismic mitigation," *Applied Sciences*, vol. 9, no. 19, p. 4096, 2019.
[26] S. Xue, J. Kang, L. Xie, R. Zhang, and X. Ban, "Cross-Layer installed cable-bracing inerter system for MDOF structure seismic response control," *Applied Sciences*, vol. 10, no. 17, p. 5914, 2020.
[27] H. Wang, H. Gao, J. Li, Z. Wang, Y. Ni, and R. Liang, "Optimum design and performance evaluation of the tuned inerter-negative-stiffness damper for seismic protection of single-degree-of-freedom structures," *International Journal of Mechanical Sciences*, vol. 212, Article ID 106805, 2021.
[28] J. P. Den Hartog, *Mechanical Vibrations*, Dover, Mineola, NY, USA, 4th edition, 1956.
[29] Y. Jiang, Z. Zhao, R. Zhang, D. De Domenico, and C. Pan, "Optimal design based on analytical solution for storage tank with inerter isolation system," *Soil Dynamics and Earthquake Engineering*, vol. 129, Article ID 105924, 2020.